International Journal of Pattern Recognition
and Artificial Intelligence
Vol. 32, No. 11 (2018) 1855019 (12 pages)

DOI: 10.1142/S0218001418550194

Calibration Method for Mapping Camera Based on a Precise Grouped Approach Method

Lina Zheng* and Guoqin Yuan†

Key Laboratory of Airborne Optical Imaging and Measurement
Changchun Institute of Optics, Fine Mechanics and Physics
Chinese Academy of Science
Changchun 130033, P. R. China
**ailsazheng@163.com*
†*13943195584@139.com*

Xue Leng

Changguang Insight Vision Opto-Electronic
Co., Ltd., Changchun 130033, P. R. China
Kramerleng@163.com

Yingfeng Wu

BMW China Service Ltd.
Shenyang 110000, P. R. China
Wuyingfeng@163.com

Received 25 January 2018
Accepted 28 March 2018
Published 18 June 2018

This paper introduces a new calibration method for the mapping camera called Precise Grouped Approach Method (PGAM). The conventional calibration method for the mapping camera is the exact measuring angle method. The accuracy of this method can be reduced by theoretical uncertainties and the number and distribution of observation points. PGAM is able to overcome these disadvantages and improve the accuracy. Firstly, we reduce the theoretical uncertainties by means of a grouped approach method, which rectifies the high-precision rotation stage to zero position. Secondly, a weighted theory is applied to eliminate the effect of the number and distribution of observation points. Finally, the accuracy of PGAM is analyzed. The experiment result shows that the calibration accuracy is significantly improved when using the proposed PGAM algorithm, compared to the conventional one under the identical experimental condition.

Keywords: PGAM; mapping camera; calibration; exact measuring angle method; weighted theory.

† Corresponding author.

1. Introduction

In convention, camera calibration plays an important role when studying the spatial location of the objects using the photogrammetric method, such as aerial mapping,[8,11,17] photogrammetry, machine vision,[3,10,12] computer vision[5] and machine production, etc. There are two typical calibration methods, i.e. model plane[17] or exact measuring angle.[2,4] The model plane method utilizes a chessboard calibration pattern. The camera takes a few pictures from different orientations. Then, nonlinear error function is resolved to calculate the inner orientation elements of the camera using the coordinates of the model plane and its image.[17] Such calibration method is more suitable for close-range cameras due to the limited size of the model plane.[8,11,17] In the exact measuring angle method, parallel light is produced by a collimator. Camera measures the incident angle of the parallel light and the coordinate of its image for calculating the inner orientation elements and the distortion parameters.[2,4] This method is more suitable for aerial cameras with longer focal length. The algorithm of the exact measuring angle method is intuitive, simple, and easy to realize. However, it can only be applied in a strict laboratory environment. Due to random error, the calculated accuracy of the inner orientation elements vary considerably with the variation of observation points, even under the same laboratory conditions.[9,13–15] Here, we propose the Precise Grouped Approach Method (PGAM), which can improve the calibration accuracy of inner orientation elements by rectifying the precision rotation stage to the principle point to reduce theoretical uncertainty, and weighted theory is applied to process corresponding data.

2. Exact Measuring Angle Method

The calibration principle of the exact measuring angle method is illustrated in Fig. 1. The camera is mounted on a precision rotation stage. At the initial rotation angle,

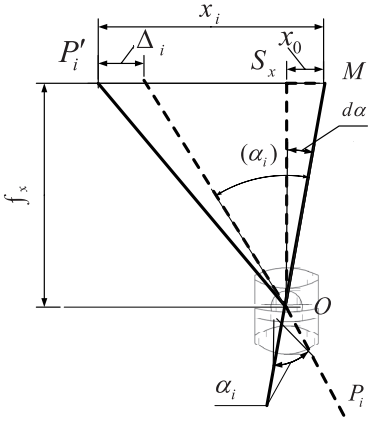

Fig. 1. Geometry of exact measuring angle method.

M is the initial coordinate of the star point image on the CCD image plane. It is set as the geometric center of the CCD image plane; O is the unknown principal point; S_x is the projection of the principal point on the camera focal plane; and OS_x is the unknown principal distance. At another rotation angle α_i, star point P_i projects itself on the CCD image plane as P_i.

According to the theory of geometrical optics, the distortion Δ_i of incident beam at angle α_i is

$$\Delta_i = x_i - x_0 - f_x \times \tan(\alpha_i - d\alpha). \tag{1}$$

Expand $\tan(\alpha_i - d\alpha)$ in Taylor series, and neglect the higher-order terms, we obtain:

$$\tan(\alpha_i - d\alpha) = \tan\alpha_i - \sec^2\alpha_i \times d\alpha. \tag{2}$$

In Eq. (2), $d\alpha = \arctan(x_0/f)$. If $x_0 \ll f$, then $d\alpha \approx x_0/f$. After simplifying, we obtain:

$$\Delta_i = x_i - f_x \tan\alpha_i + x_0 \tan^2\alpha_i. \tag{3}$$

Subsequently, rotating the precision rotation stage, we obtain several pairs of angle and image of the star points. If matrices $\boldsymbol{V}, \boldsymbol{X}, \boldsymbol{B}$ and $\boldsymbol{N}$ are respectively defined as:

$$V = \begin{bmatrix} \Delta_1 \\ \Delta_2 \\ \vdots \\ \Delta_n \end{bmatrix}, \quad X = \begin{bmatrix} x_1 \\ x_2 \\ \vdots \\ x_n \end{bmatrix}, \quad B = \begin{pmatrix} \tan\alpha_1 & -\tan^2\alpha_1 \\ \tan\alpha_2 & -\tan^2\alpha_2 \\ \vdots & \vdots \\ \tan\alpha_n & -\tan^2\alpha_n \end{pmatrix}, \quad N = \begin{bmatrix} f_x \\ x_0 \end{bmatrix},$$

then we have $V = X - BN$. The exact measuring angle method sets the constraint $PRS = \min(\sum \Delta_i^2) = \min(V^T V)$ to solve inner orientation elements. Therefore, matrix N is solved by the least-squares method $N = (B^T B)^{-1} B^T X$, i.e.

$$\begin{aligned} x_0 &= \frac{-\sum x_i \tan^2\alpha_i \times \sum \tan^2\alpha_i + \sum x_i \tan\alpha_i \times \sum \tan^3\alpha_i}{\sum \tan^2\alpha_i \times \sum \tan^4\alpha_i - \left(\sum \tan^3\alpha_i\right)^2}, \\ f_x &= \frac{\sum x_i \tan\alpha_i \times \sum \tan^4\alpha_i - \sum x_i \tan^2\alpha_i \times \sum \tan^3\alpha_i}{\sum \tan^2\alpha_i \times \sum \tan^4\alpha_i - \left(\sum \tan^3\alpha_i\right)^2}. \end{aligned} \tag{4}$$

The inner orientation elements of the camera obtained by the exact measuring angle method are indirect. Uncertainties mainly come from[4,6,7,16]:

(1) Theoretical uncertainty caused by neglecting the higher order terms of $\tan(\alpha_i - d\alpha)$ and simplifying $d\alpha$ equals to $\frac{x_0}{f}$;
(2) Angle uncertainty σ_α when acquiring observation points $p_1, p_2 \ldots, p_n$;
(3) Position uncertainty σ_x of acquiring image points $x_1, x_2, \ldots, x_n$;
(4) Environmental factors such as temperature, vibration, light sources and airflow during calibration. Providing necessary shielding against the negative effects of

the environment, the calibration accuracy of the principal point is

$$\sigma_{x0} = \sqrt{\sum_{i=1}^{n} \left(\frac{\partial x_0}{\partial x_i}\right)^2 \sigma_{x_i}^2 + \sum_{i=1}^{n} \left(\frac{\partial x_0}{\partial \alpha_i}\right)^2 \sigma_{\alpha_i}^2}. \tag{5}$$

From Eq. (4), we obtain:

$$\frac{\partial x_0}{\partial \alpha_i} = \frac{\partial x_0}{\partial \tan \alpha_i} \cdot \frac{d \tan \alpha_i}{d\alpha_i} = \frac{\partial x_0}{\partial \tan \alpha_i} \cdot \sec^2(\alpha_i). \tag{6}$$

Denote:

$$A_1 = \sum_{i=1}^{n} \left(\frac{\partial x_0}{\partial x_i}\right)^2, \quad A_2 = \sum_{i=1}^{n} \left(\frac{\partial x_0}{\partial \alpha_i}\right) \sec^2(\alpha_i).$$

Suppose the observation points have invariant errors during calibration,

$$\sigma_{\alpha 1} = \sigma_{\alpha 2} = \cdots = \sigma_{\alpha n}, \quad \sigma_{x1} = \sigma_{x2} = \cdots = \sigma_{xn},$$

then

$$\sigma_{x0} = \sqrt{A_1 \sigma_x^2 + A_2 \sigma_\alpha^2}. \tag{7}$$

Similarly,

$$\sigma_f = \sqrt{A_3 \sigma_x^2 + A_4 \sigma_\alpha^2}, \tag{8}$$

where

$$A_3 = \sum \left(\frac{\partial f_x}{\partial x_i}\right)^2, \quad A_4 = \sum \left(\frac{\partial f_x}{\partial \alpha_i}\right)^2.$$

According to $PRS = \sum_{i=1}^{n} (x_i - f_x \tan \alpha_i + x_0 \tan^2 \alpha_i)^2$, we have:

$$\sigma_{PRS}^2 = \sum \left[\left(\frac{\partial PRS}{\partial x_i}\right)^2 \sigma_x^2 + \left(\frac{\partial PRS}{\partial \alpha_i}\right)^2 \sigma_\alpha^2 + \left(\frac{\partial PRS}{\partial x_0}\right)^2 \sigma_{x0}^2 + \left(\frac{\partial PRS}{\partial f_x}\right)^2 \sigma_{f_x}^2 \right]. \tag{9}$$

In an independent calibration process, observation points $p_1, p_2, \ldots, p_n$ are fixed, A_1, A_2, A_3, and A_4 are constants, σ_{x0}, σ_f and σ_{PRESS} are also constants.

From Eqs. (5)–(9), we conclude:

(1) As a result of the theoretical error, the exact measuring angle method cannot acquire accurate solution of principal point and principal distance.
(2) By increasing only the number of observation points, we cannot consistently improve the calibration accuracy.
(3) Despite being in the same calibration environment, different observation points could result in different calibration accuracies.

PGAM is able to solve all these disadvantages.

3. Precise Grouped Approach Method (PGAM)

PGAM improves the calibration accuracy by reducing theoretical uncertainty and using weighted theory to process the approached group data. It consists of two parts:

(1) Divide the calibration into several groups. Adjust M of group $t+1$ accordingly based on the result of group t, until approaching $x_0 \to 0, d\alpha \to 0$. Then, independently calibrate group $t+1$, so that theoretical uncertainty can be reduced greatly.
(2) Due to the slight adjustment of M, the distribution of observation points of groups 1, 2, until $J+1$ is changed. Based on Eqs. (6)–(9), σ_{x0}, σ_f, PRS of each group are varied as well. In order to eliminate the influence of the redistribution of the observation points on the calibration accuracy, the PGAM algorithm applies unequal weights to each group data.

Assuming that we have data from all $J+1$ groups, the number of the observation points in each group is $\boldsymbol{n}$. For the exact measuring angle method, the solved inner orientation elements from group $\boldsymbol{t}$ are x_{0t} and f_t, the accuracies are σ_{x0t} and σ_{f_t}, the constraint is $PRS_t = \sum_{k=1}^{n} (x_{tk} - f_t \tan\alpha_{tk} + x_{0t}\tan^2\alpha_{tk})^2$, the accuracy is σ_{PRSt}, and the set weight values of P_{Et}, P_{xt}, P_{ft} for PRS_t are x_{0t} and f_t, respectively[2]:

$$P_{Et} = \frac{1}{\sigma^2_{PRSt}}, \quad P_{xt} = \frac{1}{\sigma^2_{x0t}}, \quad P_{ft} = \frac{1}{\sigma^2_{f_t}}. \tag{10}$$

For PGAM algorithm, denote the solved inner orientation elements as X_0, F_x and the constraint of group t as PRS'_t. Meanwhile, define $\bar{x}^1_0,\ \bar{f}^1_0$ as:

$$\bar{x}^1_0 = \frac{1}{\sum_{i=1}^{J+1} P_{xi}} \sum_{i=1}^{J+1} P_{xi} x_{0i}, \quad \bar{f}^1_0 = \frac{1}{\sum_{i=1}^{J+1} P_{fi}} \sum_{i=1}^{J+1} P_{fi} f_i.$$

According to the maximum likelihood theory, set $\bar{x}^1_0, \bar{f}^1_0, w^0_1, w^0_2$, respectively, as the approximation and correction values of X_0, F_x, which means

$$X_0 = \bar{x}^1_0 + w^0_1, \quad F_x = \bar{f}^1_0 + w^0_2,$$
$$PRS'_t = \sum_{k=1}^{n} (x_{tk} - (\bar{f}^1_0 + w^0_2)\tan\alpha_{tk} + (\bar{x}^1_0 + w^0_1)\tan^2\alpha_{tk})^2.$$

Neglecting the higher-order terms of the constraint, we obtain:

$$PRS'_t = \sum_{k=1}^{n} ((x_{tk} - \bar{f}^1_0 \tan\alpha_{tk} - \bar{x}^1_0 \tan^2\alpha_{tk})^2) + a_{t1} w^0_1 + a_{t2} w^0_2, \tag{11}$$

where

$$\begin{pmatrix} a_{t1} \\ a_{t2} \end{pmatrix} = \begin{pmatrix} \partial PRS'_t & 0 \\ 0 & \partial PRS'_t \end{pmatrix} \begin{bmatrix} \dfrac{1}{\partial \overline{x_0}} \\ \dfrac{1}{\partial \overline{f_0}} \end{bmatrix}.$$

Here, introducing the parameters $\overline{PRS_t}, E_t, W_t, PRS_{\sum A}, PRS_{\sum G}$, which are defined as follows, respectively:

$$\overline{PRS_t} = \sum_{k=1}^{n} (x_{tk} - \bar{f}^{\,1}_{\,0} \tan \alpha_{tk} - \bar{x}^{\,1}_{\,0} \tan^2 \alpha_{tk})^2,$$

$$E_t = PRS_t - \overline{PRS_t},$$

$$W_t = PRS'_t - PRS_t,$$

$$PRS_{\sum A} = \sum_{i=1}^{J+1} (P_{Ei} \times \left(\sum_{k=1}^{n} (x_{ik} - f_i \tan \alpha_{ik} - x_{0i} \tan^2 \alpha_{ik})^2 \right),$$

$$PRS_{\sum G} = \sum_{i=1}^{J+1} (P_{Ei} \times \left(\sum_{k=1}^{n} (x_{ik} - F_x \tan \alpha_{ik} - X_0 \tan^2 \alpha_{ik})^2 \right).$$

Then, we have:

$$W_t = a_{t1} w_1^0 + a_{t2} w_2^0 - E_t. \tag{12}$$

Thanks to the reliability of data from each group, the quadratic summation of the whole field distortion of all $J+1$ groups should have minimal variation properties after applying PGAM algorithm. This is set as the constraint condition, and we solve the correction value of X_0 and F_x.

That means w_1^0 and w_2^0 should meet:

$$\min \left(\sum_{i=1}^{J+1} P_{Ei} W_t^2 = \left(PRS_{\sum A} - PRS_{\sum G} \right)^2 \right).$$

Define matrices W, A, w^0, L, P as:

$$W = \begin{bmatrix} W_1 \\ \vdots \\ W_{J+1} \end{bmatrix}, \quad A = \begin{pmatrix} a_{11} & a_{12} \\ \vdots & \vdots \\ a_{(J+1)1} & a_{(J+1)2} \end{pmatrix}, \quad w^0 = \begin{pmatrix} w_1^0 \\ w_2^0 \end{pmatrix},$$

$$L = \begin{bmatrix} E_1 \\ \vdots \\ E_{J+1} \end{bmatrix}, \quad P = \begin{pmatrix} P_{E1} & 0 & 0 \\ \vdots & \ddots & \vdots \\ 0 & 0 & P_{EJ+1} \end{pmatrix}.$$

From Eq. (12), we have $W = Aw^0 - L$.

The equation is simplified according to the constraint condition $\min(W^T PW)$ of the PGAM algorithm,

$$A^T PW = 0. \tag{13}$$

The solution is $w^0 = (A^T PA)^{-1} A^T PL$, i.e.

$$w_1^0 = \frac{\sum_{i=1}^{j+1} p_{Ei} a_{i2}^2 \sum_{i=1}^{j+1} p_{Ei} a_{i1} E_i - \sum_{i=1}^{j+1} p_{Ei} a_{i1} a_{i2} \sum_{i=1}^{j+1} p_{Ei} a_{i2} E_i}{\sum_{i=1}^{j+1} p_{Ei} a_{i1}^2 \sum_{i=1}^{j+1} p_{Ei} a_{i2}^2 - \left(\sum_{i=1}^{j+1} p_{Ei} a_{i1} a_{i2}\right)^2},$$

$$w_2^0 = \frac{\sum_{i=1}^{j+1} p_{Ei} a_{i1}^2 \sum_{i=1}^{j+1} p_{Ei} a_{i2} E_i - \sum_{i=1}^{j+1} p_{Ei} a_{i1} a_{i2} \sum_{i=1}^{j+1} p_{Ei} a_{i1} E_i}{\sum_{i=1}^{j+1} p_{Ei} a_{i1}^2 \sum_{i=1}^{j+1} p_{Ei} a_{i2}^2 - \left(\sum_{i=1}^{j+1} p_{Ei} a_{i1} a_{i2}\right)^2}.$$

In order to eliminate the uncertainty caused by ignoring the higher order terms of Eq. (11), we use the iteration method to approach the true value of X_0, F_x. When $|w^r - w^{r-1}| < \varepsilon$ (ε is the approaching accuracy), it is considered as the final solution.

The distortion coefficient can be obtained using the distortion pattern of Refs. 1 and 18.

$\sum_{i=1}^{J+1} P_i W_i^2/\sigma^2$ obeys the χ^2 distribution with $(J+1-2)$ degrees of freedom.[1] We use $\sum_{i=1}^{J+1} P_i W_i^2/(J-1)$ as the unbiased estimator of σ^2. Therefore, the standard uncertainty of PGAM algorithm and uncertainty of inner orientation elements are given respectively:

$$u = \sum_{i=1}^{J+1} P_i W_i^2/(J-1),$$

$$\begin{bmatrix} u_{X_0} \\ u_{Fx} \end{bmatrix} = u \begin{bmatrix} \sqrt{d_{11}} \\ \sqrt{d_{12}} \end{bmatrix},$$

where d_{11} and d_{12} are diagonal elements of the matrix $(A^T PA)^{-1}$.

The PGAM flowchart is illustrated in Fig. 2 as follows

Step 1. When $i = 1$, set the geometrical center of the CCD image plane as the original coordinate data of M, when $i \neq 1$, adjust the coordinate data of M according to data of group $i-1$. Adjust the angle of the precision rotation stage, record the angle data and the image position, and then confirm matrices X and B.

Step 2. Calculate the inner orientation elements as per Eq. (4), calculate PRS, and then calculate σ_{x0}, σ_f and σ_{PRESS} as per Eqs. (7)–(9).

Step 3. Judge the inner orientation elements of matrices N and $d\alpha$ acquired from Step 2, to see whether the accuracy could meet the requirement or not. If so, proceed to Step 4; otherwise revert to Step 1.

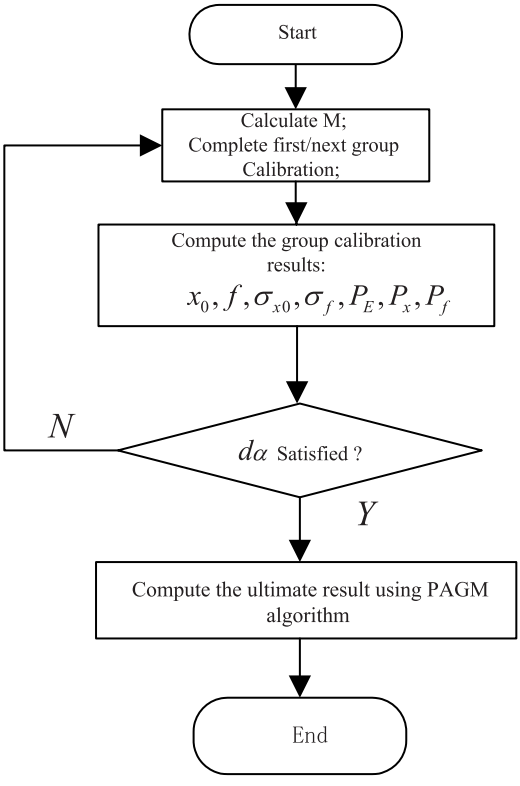

Fig. 2. Flowchart of the PGAM.

Step 4. Adopt the PGAM algorithm to solve different groups of data, acquire the optimal estimator of the intrinsic parameters, and finally complete the process.

From the process, we determine that steps 1–3 decrease the theoretical uncertainty by approaching the truth value of intrinsic parameters. Step 4 decreases the effect on calibration accuracy from the distribution status of the observation points by the PGAM algorithm.

4. Experiment Results and Analysis

PGAM algorithm is verified in the laboratory. First, set the image geometrical center as the original coordinate data of M, and achieve the first group data. In accordance with the process set out in Fig. 2, suppose that $d\alpha < 3.5 \times 10^{-4}$ rad, $\varepsilon = 1 \times 10^{-5}$.

The experiment setup is illustrated in Fig. 3, including a star tester, a collimator, a precision rotation stage, and a mapping camera. The photo of the measurement system and the image of the star point are given in Fig. 4. The focal length of the collimator is 1600 mm. The accuracy of the precision rotation stage is $\sigma_\alpha = 0.5''$.

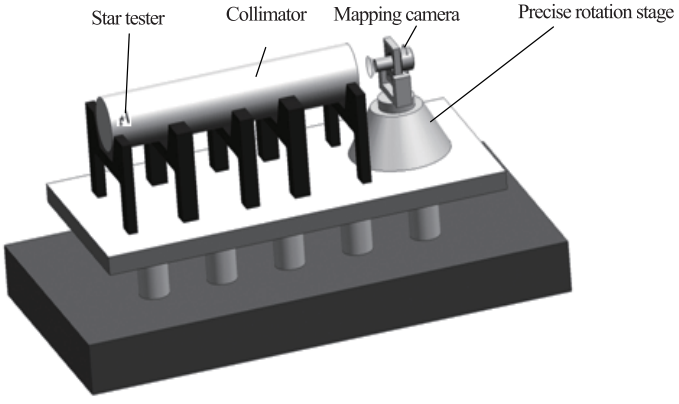

Fig. 3. Schematics of the measurement system.

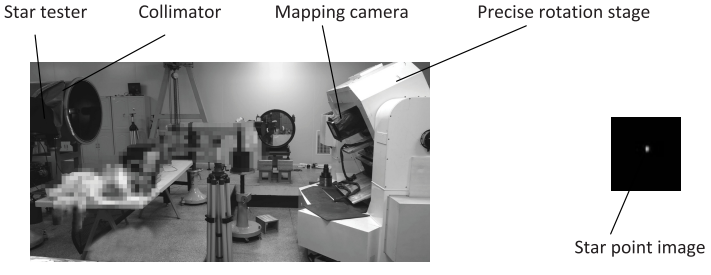

Fig. 4. Photo of the measurement system and image of the star point.

The accuracy of the image point position is $\sigma_x = 0.8\,\mu$m, and the number of observation points in each group is $\mathbf{n} = 30$.

Processing the data in Table 1, we obtain[18]:

$$PRS_{\sum A} = 24.939$$

$$P_{E1} : P_{E2} : P_{E3} : P_{E4} = 1 : 1.18 : 1.43 : 1.69,$$

$$\bar{\sigma}_{x0} = \frac{1}{J+1}\sum_{i=1}^{J+1} \sigma_{x0}(i) = 7.275,$$

Table 1. Results of measurement adopting PGAM.

Grouped Sequence	$d\alpha \times 10^{-4}$ (rad)	$\sigma_{x0}(i)$ (μm)	$\sigma_f(i)$ (μm)	$\sum_{i=1}^{n} \Delta_i^2$ (μm)
$i = 1$	26	7.2	12.2	4.5
$i = 2$	9.8	8.7	13.4	5.5
$i = 3$	6.0	6.8	11.8	4.2
$i = 4$	2.7	6.4	10.9	4.7

$$\bar{\sigma}_f = \frac{1}{J+1}\sum_{i=1}^{J+1}\sigma_f(i) = 12.075,$$
$$u_{X_0} = 2.12\,\mu\text{m}, \quad u_{F_x} = 4.02\,\mu\text{m},$$
$$\nu = \frac{\bar{\sigma}_{x0} - u_{X0}}{\bar{\sigma}_{x0}} \times 100\% = 70.9\%,$$
$$\lambda = \frac{\bar{\sigma}_f - u_{F_x}}{\bar{\sigma}_f} \times 100\% = 66.7\%.$$

The experiment results are shown in Table 1. $\sigma_{x0}(i)$ and $\sigma_f(i)$ represent the calibration accuracy of the principal point and principal distance in group $\boldsymbol{i}$ in terms of the traditional method. ν and λ represent the improvement percentage of calibration accuracy of the principal point and principal distance, after comparing the PGAM algorithm with the exact measuring angle method.

5. Conclusions

PGAM is proposed to improve the calibration accuracy of the intrinsic parameters of the mapping camera. It reduces the theoretical uncertainties and eliminate effects of the distribution status of the observation points. Experiment results show that, provided $n = 30$ observation points of each group, the average percentage improvement in calibration accuracies of the principal point and principal distance are 70.9% and 66.7%, respectively. Therefore, the PGAM algorithm is capable of precise calibration of inner orientation elements in the laboratory with higher accuracy.

References

1. M. Bauer *et al.*, Geometrical camera calibration with diffractive optical elements, *Opt. Exp.* **16**(25) (2008) 20241–20248.
2. L. Bo, J. Jiqiang and D. Yalin, Geometric calibration with angle measure for CCD aerial photogrammetric camera in laboratory, *Laser and Infrared* **40**(3) (2010) 298–301.
3. T. D'Orazio and C. Gudragnella, A survey of automatic event detection in multi-camera third generation surveillance systems, *Int. J. Pattern Recognit. Artif. Intell.* **29**(1) (2015) 1555001.
4. W. Guodong, H. Bing and H. Xun, Calibration of geometric parameters of line-array CCD camera based on exact measuring angle in lab, *Opto-Electron. Eng.* **15**(10) (2007) 1628–1632.
5. R. Hartley and A. Zisserman, *Multiple View Geometry in Computer Vision*, 2nd edn. (Cambridge University Press, 2003).
6. F. Hong and Y. Baozong, High performance camera calibration algorithm, *SPIE* **2067** (1993) 1–13.
7. J.-S. Lee and Y.-H. Jeong, CCD camera calibrations and projection error analysis, *IEEE Int. Conf. Sci. Technol.* **2**(2) (2000) 50–55.
8. R. K. Lenz and R. Y. Tsai, Techniques for calibration of the scale factor and image center for high accuracy 3D machine vision metrology, *IEEE Trans. Pattern Anal. Mach. Intell.* **PAMI-10** (1988) 713–720.

9. L. Weiyi *et al.*, Calibration of inner orientation elements for camera by means of star points, *Opto-Electron. Eng.* **18**(9) (2010) 2086–2089.
10. L. Qin and T. Wang, Improved position and attitude determination method for monocular vision in vehicle collision warning system, *Int. J. Pattern Recognit. Artif. Intell.* **30**(7) (2016) 1655019.
11. R. Y. Tsai, A versatile camera calibration technique for high accuracy 3D machine vision metrology using off-the-shelf TV cameras and lenses, *IEEE JRA* **3**(4) (1987) 323–344.
12. H. Wang, A shape-aware road detection method for aerial images, *Int. J. Pattern Recognit. Artif. Intell.* **31**(4) (2017) 1750009.
13. W. Zhihe *et al.*, New method of CCD camera calibration based on collimator, *J. Infrared Millim. Waves* **26**(6) (2007) 465–470.
14. W. Zhizhuo, *The Principle of Photogrammetry* (Wuhan University Press, Wuhan, 2007), pp. 240–253.
15. L. Weiyi *et al.*, Measurement error impact on parameters calibration in precise angle measurement method, *Infrared Laser Eng.* **38**(4) (2009) 705–709.
16. M. Yingtai, *Error Theory and Precision Analysis* (National Defence Industry Press, Beijing, 1982), pp. 20–230.
17. Z. Zhang, A flexible new technique for camera calibration, *IEEE Trans. Pattern Anal. Mach. Intell.* **PAMI-22** (2000) 1330–1334.
18. D. Zhenliang, *Error Theory and Data Processing* (Harbin Institute of Technology Press, Harbin, 2006), pp. 46–184.

Lina Zheng is an Associate Researcher in Changchun Institute of Optics Fine Mechanics and Physics, and also a Supervisor of Postgraduate in the University of the Chinese Academy of Sciences. She received her BS degree in Electronics from the Jilin University in 2003, and her MS degree in Mechatronics from the University of the Chinese Academy of Sciences in 2008. She received her Ph.D. degree in Optical Engineering from the University of the Chinese Academy of Sciences in 2013. Her current research interests include Optical Imaging and Mapping Techniques for Aerial Remote Camera.

Guoqin Yuan received his MS degree from the Jilin University in 2007 and the Ph.D. degree in Optical Engineering from The University of the Chinese Academy of Sciences in 2012. He is now an Associate Researcher in Changchun Institute of Optics Fine Mechanics and Physics. His current research interests include Optical Imaging and Mapping Techniques for Aerial Remote Camera.

Xue Leng received his BS degree from the Dalian Maritime University in 1999, and his MS degree from the Changchun University of Science and Technology in 2007. He is now an Associate Researcher in Changguang Insight Vision Opto-electronic Co., Ltd. His current research interests include Aerial Photoelectric Detection.

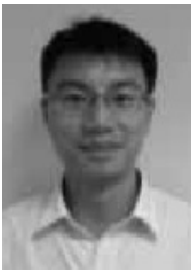

Yingfeng Wu received his MS degree from the Jilin University in 2007. He is now working in BMW China Service Ltd. Company. His current research interests cover calibration method of mapping camera.